CrossMark

ARTICLE

Directionally solidified Al_2O_3/ZrO_2 eutectic ceramic prepared with induction heating zone melting

Weinan Wang, Juncheng Liu,[a] and Caiyu Song
School of Materials Science and Engineering, Tianjin Polytechnic University, Tianjin 300387, China

(Received 26 January 2018; accepted 10 April 2018)

To prepare high quality large solidified Al_2O_3/ZrO_2 eutectic ceramic, the preparation processing of the presintered ceramic as a feed rod was investigated via experiments; some parameters of the induction heating zone process were optimized via numerical modeling; an Al_2O_3/ZrO_2 eutectic ceramic rod with a diameter 10 mm was prepared. The results show that increasing the sintering temperature could increase the presintered ceramic's bulk density, while increasing sintering time had little effect. And the bulk density increased first and then decreased with the molding pressure increase. And the saucer coil obtained a higher temperature gradient than the tubbiness coil for a fixed crucible wall maximum temperature, and the coil turn's increase could increase the melting zone height in the induction zone melting process. In the directionally solidified Al_2O_3/ZrO_2 eutectic ceramics, Al_2O_3 phase is the matrix phase, and the ZrO_2 phase embedded in the Al_2O_3 phase mostly with the rod shape, and little with lamellar. The hardness of directionally solidified eutectic ceramics reaches 16.17 GPa and the fracture toughness reaches 4.76 MPa $m^{1/2}$, which are 1.7 times and 1.5 times of the presintered eutectic ceramic, respectively.

I. INTRODUCTION

Directionally solidified eutectic oxide ceramics are promising to be a new generation of ultra high temperature structural materials for aerospace engines due to their unique high temperature mechanical properties and ablation resistance. Since the 21st century, the demand for ultra high temperature (≥1650 °C) materials has being become more and more urgent with the rapid development of the aerospace industry. Ultra high temperature materials with excellent properties could make the engine and turbine work normally at ultra-high temperature without a cooling system, thus promote fuel combustion and reduce consumption and harmful emissions. Compared with the high-performance ceramics prepared by the traditional sintering method, there are no pores and interface amorphous phases in the directionally solidified eutectic ceramics, thus the material's mechanical properties improve greatly, especially at high temperatures, thus is very promising to be a new generation of ultra high temperature structural materials.[1] In recent years, scholars from various countries have carried out a lot of research studies. They prepared directionally solidified eutectic ceramics with different experimental methods. In 1997, Waku et al.[2–4] prepared an $Al_2O_3/Y_3Al_5O_{12}$ (YAG) eutectic ceramic with excellent high temperature performance using an improved Bridgeman method. This ceramic's tensile strength at 1700 °C was up to 160 MPa, and its elongation was up to 10%. At 1600 °C, the material was applied 10^{-4}/s strain rate; its creep strength could be as high as 433 MPa, which is 13 times of the sintered ceramic with the same composition. After zirconia doping, $Al_2O_3/Y_2O_3/ZrO_2$ eutectic ceramics had the flexural strength at 1600 °C as high as 851 MPa, which was 57 times of the same composition sintered ceramics.[5] Su et al.[6] prepared $Al_2O_3/GdAlO_3/ZrO_2$ eutectic ceramic with laser floating zone melting having a higher temperature gradient. The sample was rather small and showed an irregular outline due to the spot diameter's limit. Omar et al.[7] prepared $Al_2O_3/Y_3Al_5O_{12}/ZrO_2$ eutectic ceramic with the microdrawing method, which was of very high strength and small size. Combustion synthesis was also used to prepare Al_2O_3/ZrO_2 (Y_2O_3) eutectic ceramics.[8,9] This method had a very high solidification rate resulting in great differences of both the phase components and the microstructures.

The induction heating zone melting (IHZM) method is of a high temperature gradient and able to prepare regular shape large samples. The higher the temperature gradient in front of the solid–liquid interfaces during the solidification process, the more homogeneous and compact the structure of the solidified ceramic, the better mechanical properties the ceramic.[10] Generally, the preparation of solidified eutectic ceramic requires high density presintered eutectic samples as the starting materials, which could be prepared with the conventional sintering in a muffle furnace, hot pressing sintering,[11] reactive

[a]Address all correspondence to this author.
e-mail: jchliu@tjpu.edu.cn
DOI: 10.1557/jmr.2018.113

 © Materials Research Society 2018

https://doi.org/10.1557/jmr.2018.113 Published online by Cambridge University Press

sintering,[12] and microwave sintering method.[13] In the case of complex shape and large volume sample, the conventional sintering method is commonly used.

Here, the presintered eutectic ceramic rod was first prepared by the conventional sintering in this paper. The effects of sintering temperature, sintering time, and molding pressure on the bulk density and porosity of the presintered body were studied. Next, Al_2O_3/ZrO_2 eutectic ceramic was prepared with IHZM. The effects of coil shape and number of turns on the temperature distribution of the crucible, as well as the effect of the maximum crucible wall temperature on the solidified eutectic ceramic morphology were investigated. And the solidification structure and mechanical property of the ceramic were also analyzed and discussed.

II. EXPERIMENTAL DETAILS

A. Preparation of presintered ceramics

According to the eutectic phase diagram of Al_2O_3/ZrO_2,[14] Al_2O_3, and ZrO_2 mole fractions at the eutectic point are 61.9%, 38.1%, respectively, the mass ratio of Al_2O_3:ZrO_2 is 57.4:42.6 and the eutectic temperature is 1865 °C.

Commercially available high-purity Al_2O_3, ZrO_2 powders (>3 N, 5 μm, from Beijing Fuxingkai Photo-Electric Technology Co., Ltd., Beijing, China) were the starting materials. Concentration of 5% polyvinylalcohol as a binder material was mixed with the powders uniformly, of which the mass ratio of Al_2O_3:ZrO_2 is 57.4:42.6. An amount of anhydrous ethanol was subjected to ball milling as the dispersant, followed by drying at 70 °C for 24 h. The powder was pressed into rods of Φ 10 × 20 mm with the molding method. Thereafter, three group experiments were set up to prepare presintered rods with a high bulk density and a low porosity. All parameters are listed in Table I.

B. Preparation of Al_2O_3/ZrO_2 eutectic ceramics by IHZM

Al_2O_3/ZrO_2 binary eutectic ceramics have a melting point of 1865 °C so the selected crucible material melting point must be much higher than 1865 °C. The tungsten crucible is well qualified. It can provide a temperature gradient of up to 470 °C/cm as can be seen in Ref. 15 at the solid–liquid interface, about 4–6 times the conventional Bridgman method.[16] The presintered ceramic rod was put into a vertical tungsten crucible, placed into the chamber evacuated to 1×10^{-4} Pa. When the high frequency power was put on, a high temperature belt on the crucible wall came into being, melting the inner presintering rod. As the crucible lowered vertically at a rate of 3 mm/h, the presintered rod melted and solidified bit by bit from the down to up. The influences of the coil shape and the coil turns on the temperature distribution of the crucible were simulated with the finite element method. And the coil shape and turns were determined in advance. The maximum temperature on the crucible wall was set to 2050, 2200, and 2350 °C, respectively. Based on the simulation results and the previous experimental process, the optimum process parameters for Al_2O_3/ZrO_2 eutectic ceramic preparation with IHZM were determined.

TABLE I. Experimental parameters for the sintering eutectic ceramics.

	Group 1	Group 2	Group 3
Sintering temperature (°C)	1350, 1400, 1450, 1500	1500	1500
Sintering time (h)	2	2, 3, 4	2
Molding pressure (MPa)	10	10	10, 15, 20, 25

C. Characterization

The sample phase compositions were determined with an X-ray diffractometer (XRD; D/MAX-RB, Rigaku, Tokyo, Japan; Cu $K_{\alpha 1}$, $\lambda = 0.15405$ nm) at a scanning speed of 10°/min and an energy dispersive spectrometer (EDS). The sample microstructure was observed by scanning electron microscopy (SEM; JSM-6390, JEOL Ltd., Tokyo, Japan). The sample hardness at room temperature was measured with a Vickers hardness tester (HVS-5, Yantai Huayin Experimental Instrument Co., Ltd., Yantai, China.) with a load of 9.8 N lasting 15 s, and its fracture toughness was calculated by the indentation method. At least five valid indentations were conducted on each sample cross section.

The bulk density and porosity of the presintered ceramics were determined with the Archimedes principle. Take out the sample from the dryer and dry it for 5 h in an oven at 80 °C, and then cool it down to room temperature in the oven, weigh its mass D with an electronic balance (accurate to 0.001 mg, the same as below). Next, boil the sample in water for 2 h, then cool it to room temperature, leave it in water for 24 h; after that, take it out from the water, wipe its surface water stains, and weigh its mass W. Next, suspend it in water, weigh its mass S in the water. Its density is calculated with $\rho = D/(W - S)$, and its porosity is calculated with $P = (W - D)/(W - S)$.

III. RESULTS AND DISCUSSION

A. Process parameters for presintered ceramics

1. Sintering temperature

The effects of the sintering temperature on the bulk density and porosity of the sintered ceramic are shown in Fig. 1(a). It can be seen that with the increase of the sintering temperature, the bulk density of the presintered

https://doi.org/10.1557/jmr.2018.113 Published online by Cambridge University Press

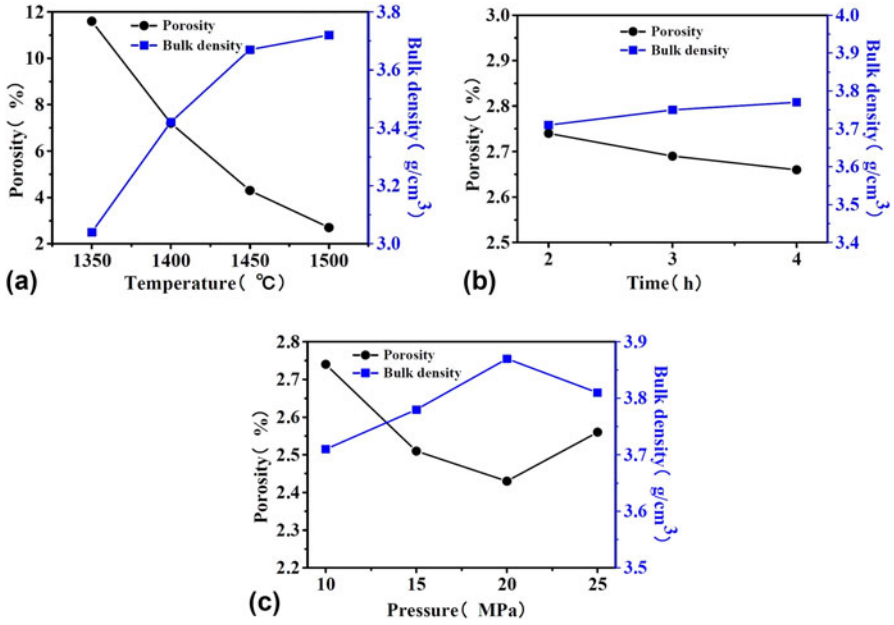


FIG. 1. Influences of the processing parameters on the samples' density and porosity. (a) Sintering temperature (10 MPa, 2 h); (b) sintering time (10 MPa, 1500 °C); (c) molding pressure (1500 °C, 2 h).

ceramic gradually increases and reaches the maximum value at 1500 °C. The porosity decreases with the increase of sintering temperature and reaches a minimum value at 1500 °C. The sintering temperature increase contributed to the mass transfer and grain growth, thus made the structure more compact.[17]

2. Sintering time

Figure 1(b) shows the effects of the sintering time on the porosity and bulk density of the presintered ceramic. It can be seen that increasing the sintering time just has a little effects on the porosity and bulk density, which are almost negligible. The sintering time doubled from 2 to 4 h, but the bulk density only increased by 0.06 and the porosity just reduced by 0.08. From the aspect of cost reduction, the sintering time of 2 h was acceptable.

3. Molding pressure

The effects of molding pressure on the bulk density and porosity of the presintered ceramics are shown in Fig. 1(c). It is clear that with the molding pressure increase, the sample porosity decreased first and then increased, while the bulk density increased first and then decreased. It is reasonable that the density increased with the molding pressure. Under the pressure of 25 MPa, the obvious layer cracks appeared on the individual body. After sintering at 1500 °C, the sample had more cracks, which might be attributed to ZrO_2 phase transformation from the monoclinic phase to tetragonal phase at 1170 °C, resulting in a volume change.[18] Therefore, the presintering rod density decreased from a macro point of view. By contrast, the sintered samples molded at 20 MPa pressure had no macro crack and had the lowest porosity and the highest bulk density. From all above, the optimum parameters for the presintered ceramic rod were as follows: the sintering temperature is 1500 °C, the sintering time is 2 h, and the molding pressure is 20 MPa.

B. Preparation of Al_2O_3/ZrO_2 eutectic ceramics by IHZM

1. Induction coil shape and number of turns

In the induction heating process, the commonly used induction coil has two shapes: one saucer shape, the other tubbiness shape. They produce different temperature distributions on the crucible wall. Figures 2(a) and 2(b) show the crucible wall temperature profiles for these two shapes of coils, of which the number of turns is 3. It can be seen that the crucible melting zone heated by the saucer coil is narrower than that by the tubbiness coil when the crucible wall maximum temperature reached 2200 °C. In other words, the crucible temperature gradient of the former is higher than that of the latter. The temperature gradient by the saucer-shaped coil was calculated to be 505 °C/cm and the temperature gradient by the tubbiness coil was only 365 °C/cm. In the directionally solidified process, a high temperature gradient favors the refinement of the grains, resulting in a better microstructure of the eutectic ceramics.[19,20] Therefore, to obtain a higher temperature gradient, the induction heating coil should be saucer-shaped.

https://doi.org/10.1557/jmr.2018.113 Published online by Cambridge University Press

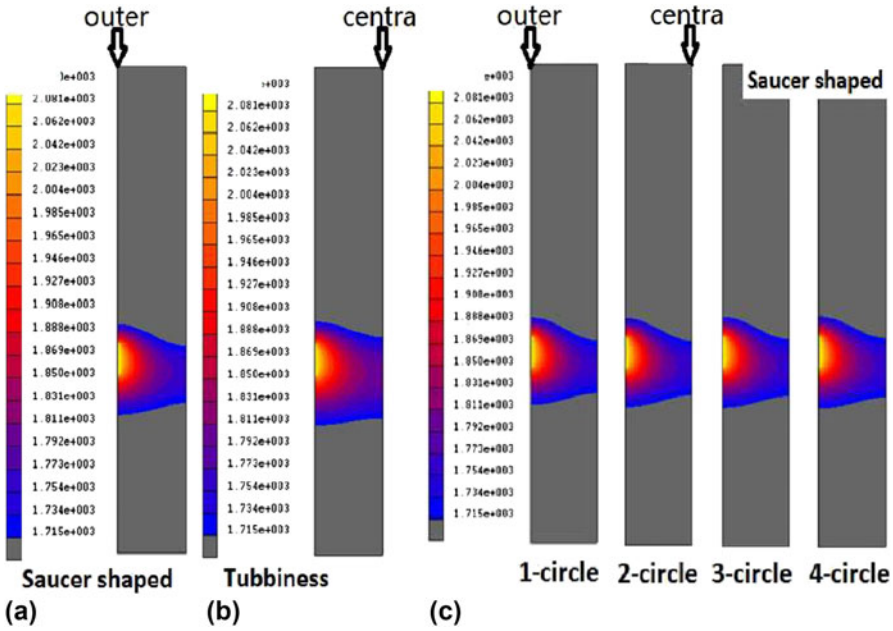


FIG. 2. Influences of the coil shape and circle number on the crucible temperature field. (a) Saucer-shaped coil with 3 turns; (b) tubbiness coil with 3 turns; (c) saucer coil with 1–4 turns, respectively.

The influence of the coil turns or circles on the temperature distribution is shown in Fig. 2(c). It can be seen that with the turns' increase, the height of the melting zone increased slowly from 9 to 12 mm. However, the temperature gradient in the growth direction interface changed little, almost kept constant about 500 °C/cm. From the component's uniformity and microstructure refinement, a narrower melting zone would be preferable under the same temperature gradient. Nevertheless, it was found in actual experimental processes that the power consumed by a single-turn coil was nearly twice of that by a three-turn coil when the crucible wall temperature reached 2200 °C. In view of the two aspects of melting zone height and power consumption, a three-turn coil was preferable.

2. Effect of maximum temperature of crucible wall on the morphology of eutectic ceramics

Figure 3 shows the macroscopic morphologies of directionally solidified eutectic ceramics prepared at 2050, 2200, and 2350 °C, respectively. As can be seen from Fig. 3(a), the presintered ceramics was not completely melted, the sample outer layer, near the crucible wall, was relatively dense, but the sample central region seemed as the presintered rod. Though the crucible wall temperature 2050 °C was higher than the eutectic melting point of 1865 °C near 190 °C, the sample center temperature was still below the eutectic melting point due to the low heat conductivity of the sample, which led to a rather large temperature gradient. When the crucible wall temperature reached 2350 °C, the presintered ceramic sample completely melted, but the crucible volatilization was very serious, a large quantity of tungsten atoms diffused into the sample, thus the sample displayed gray-black. In other words, the ceramic was polluted seriously; see Fig. 3(c). When the crucible wall temperature took 2200 °C, the presintered sample melted completely, and a dense solidified rod was obtained, with neither any macropore nor any tungsten pollution, see Fig. 3(b). Therefore, 2200 °C was suitable to the zone melting processing.

Figure 4 shows a solidified eutectic ceramic sample with a size Φ 9.94 × 22.7 mm. Its outer surface is smooth and there are no obvious pores. The little black spots might be resulted from the diffusion of a small amount of tungsten atoms.

C. Microstructure and mechanical properties

1. Phase composition and microstructure

Figure 5 shows the XRD patterns of presintered ceramics and zone melting Al_2O_3/ZrO_2 eutectic ceramics. It is clear that there is no phase component change before and after directional solidification. The solidified ceramic is also composed of Al_2O_3 and ZrO_2 phases, just the same as that of the sintered one. In the XRD pattern of the solidified ceramic, the highest peak could be indexed to (111) lattice planes of the Al_2O_3 phase ($2\theta = 34.206°$) and (122) lattice planes of the ZrO_2 phase ($2\theta = 34.733°$), the secondary high peak could be indexed to (002) lattice planes of the Al_2O_3 phase ($2\theta = 55.060°$)

https://doi.org/10.1557/jmr.2018.113 Published online by Cambridge University Press

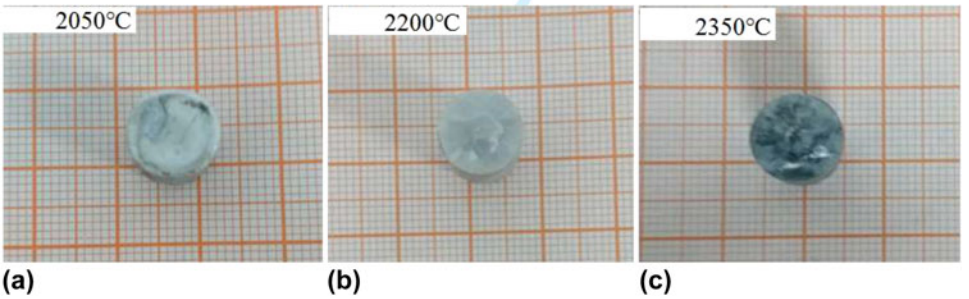


FIG. 3. Influence of the temperature on the solidified eutectic ceramic appearance (3 mm/h).

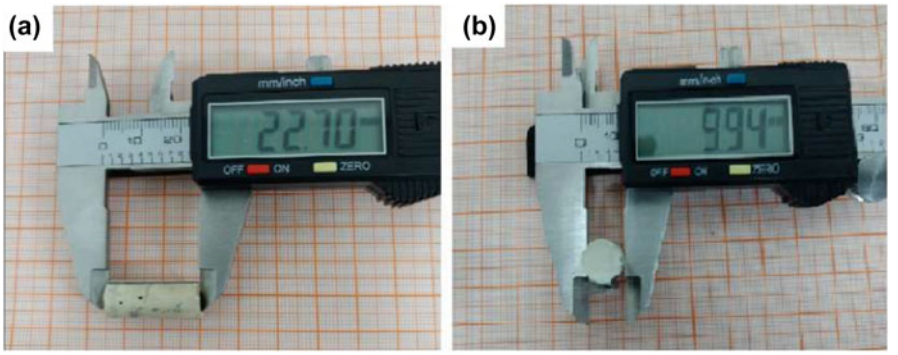


FIG. 4. Solidified eutectic ceramic's photos (2200 °C, 3 mm/h). (a) Length of the solidified eutectic ceramic; (b) diameter of the solidified eutectic ceramic.

and (204) lattice planes of the ZrO_2 phase (2θ = 55.882°), and the third high peak could be indexed to (252) lattice planes of the ZrO_2 phase (2θ = 71.884°). It is obvious that after directional solidification, the number of characteristic diffraction peaks was significantly reduced and the intensity of the diffraction peaks significantly increased, whether it was Al_2O_3 or ZrO_2 phase. That is to say, both alumina and zirconia had obvious crystallizing preference orientation during the solidification process. Compared with the sintered ceramics, the crystallinity of the directionally solidified ceramic had been greatly improved.

Figure 6(a) shows the microstructure of the presintered ceramic, which presents a typical polycrystalline ceramic morphology. The grains are randomly distributed without any orientation, and pores can be seen everywhere. Both the grain boundary and pore are the key factors affecting the mechanical properties of ceramic materials.[21] The more the grain boundaries and pores, the worse the mechanical properties of ceramics.

Figures 6(b) and 6(c) show the cross-section microstructure and the longitudinal one of the zone melting Al_2O_3/ZrO_2 eutectic ceramic, respectively. Figure 6(d) shows that the region 1 contains two elements of Zr and O, and the region 2 contains two elements, Al and O. Based on the XRD pattern of Fig. 5 and the EDS spectrum of Figs. 6(d) and 6(e), it can be confirmed that

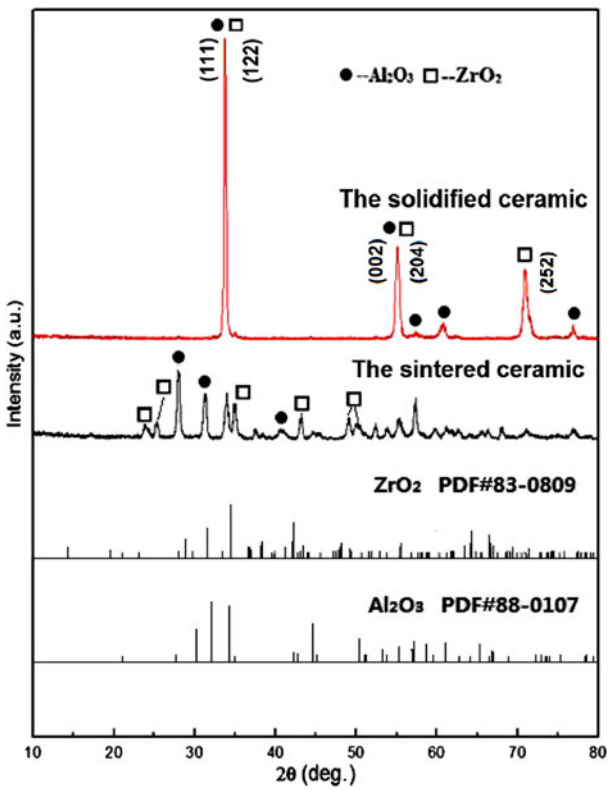


FIG. 5. XRD patterns of the directionally solidified eutectic ceramic (2200 °C, 3 mm/h) and the presintered ceramic (1500 °C).

https://doi.org/10.1557/jmr.2018.113 Published online by Cambridge University Press

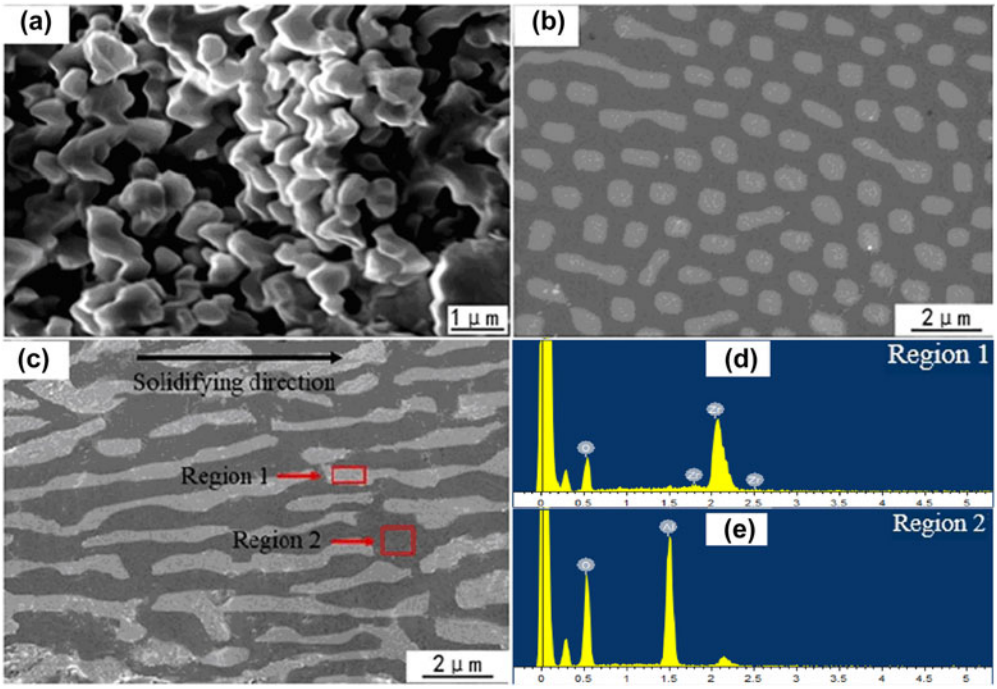


FIG. 6. Microstructures of both the presintered ceramic and the solidified ceramic. (a) Presintered ceramic, 20 MPa, 1500 °C, 2 h; (b) and (c) cross section and the longitudinal section of the solidified ceramic, 2200 °C, 3 mm/h; (d) and (e) EDS spectra analysis of the solidified ceramic.

the black phase is the Al_2O_3 phase and the gray phase with the regular distribution is the ZrO_2 phase. According to the molar fraction ratio of eutectic point Al_2O_3 and ZrO_2 and their respective densities, and the volume fraction of the Al_2O_3 phase is roughly 66.5% and the volume fraction of ZrO_2 phase is 33.5%. It can be seen from Figs. 6(b) and 6(c) that the Al_2O_3 phase is the matrix phase and most of the ZrO_2 phase is evenly embedded in the Al_2O_3 phase with rod shape, and some of the rods are connected into a thick lamellar. As can be seen from Fig. 6(b), the cross-section, the ZrO_2 phase appears as a rectangular or nearly rectangular shape. And in the longitudinal section, the ZrO_2 phase appears as a strip or rod shape, and the arrangement direction is approximately the same as the direction of the zone melting; please see Fig. 6(c).

The eutectic eigenstructure is closely related to the growth pattern of the crystal. According to Jackson–Hunt theory, the growth mode takes nonfaceted phase growth, and the eutectic microstructure presents a regular eutectic morphology when the melting entropy of the eutectic phase is less than $2R$. When both of two phases' melting entropies are greater than $5R$, the eutectic microstructure is inclined to grow at facet phases under the influence of the interface growth kinetics. When the melting entropy is greater than $2R$ and less than $5R$, the eutectic growth is a little complex, it includes both regular eutectic and irregular eutectic.[22–24]

In the Al_2O_3/ZrO_2 eutectic ceramic system, the melting entropy of the ZrO_2 phase is $3.55R$[25] [R = 8.314 J/(mol K), the molar gas constant] between $2R$ and $5R$, which is much less than that of the Al_2O_3 phase, $5.74R$.[26] And the ZrO_2 phase growth will be more prominent and priority.[10] It would grow first as a leading phase, and the Al_2O_3 phase would follow it. Therefore, the ZrO_2 phase has a tendency to grow at nonfaceted phase, and the Al_2O_3 phase prefers to grow at faceted phase. The Al_2O_3/ZrO_2 binary eutectic microstructure should be composed of regular ZrO_2 phase and irregular Al_2O_3 phase.

ZrO_2 phase volume fraction, 33.5%, is slightly greater than $1/\pi$, so most of the ZrO_2 phase is rod-like growth, the other is lamellar. Compared with Al_2O_3/ZrO_2 eutectic ceramic prepared with the explosion synthesis method,[27] herein the solidified eutectic microstructure with the induction is more uniform and has no segregation. This might be due to the very slow solidification rate, much smaller than that of the explosive synthesis method, which results in a thorough solute transport in the front of the solid–liquid interface during solidification.

2. Mechanical properties

The indentation size and the crack length were measured by using a laser scanning confocal microscope. The Vickers hardness method was used to measure the hardness values of both the presintered ceramic and the directionally solidified one, and their fracture toughness values, K_{IC}, were calculated by using formula (3-1) according to their indentations. According to the

https://doi.org/10.1557/jmr.2018.113 Published online by Cambridge University Press

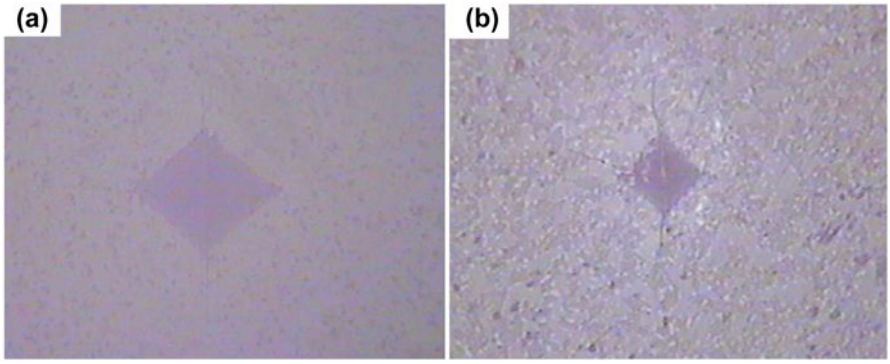


FIG. 7. Indentation morphologies. (a) Presintered ceramics (1500 °C, 2 h); (b) solidified ceramic (2200 °C, 3 mm/h).

indentation geometry, the indentation cracks can be classed into two types: Median and Palmqvist. For a Median crack, $2.5 \leq c/d$ and the fracture toughness K_{IC} is calculated using formula (3-1), Anstis formula. For a Palmqvist crack, $0 \leq c/d \leq 2.5$ and the fracture toughness K_{IC} is calculated using Niihara formula.[28] Here is the case of the Median crack.

$$K_{IC} = 0.016 \times \left(\frac{E}{H_V}\right)^{\frac{1}{2}} P c^{-\frac{3}{2}} \quad , \qquad (3\text{-}1)$$

where H_V is the Vickers hardness (GPa), l is the extended length of the crack along the diagonal, $2a$ is the diagonal length of the indentation, and $c = l + a$ (μm); E is the elastic modulus of the material, calculated by the following formula, about 320 GPa.[29]

$$E = \sum E_X V_X \quad , \qquad (3\text{-}2)$$

where E_X is the elastic modulus of each phase and V_X is its volume fraction.

Figure 7 shows the indentation morphologies for the presintered ceramics (1500 °C, 2 h), and the solidified ceramic (2200 °C, 3 mm/h). The solidified ceramic's hardness and fracture toughness are 16.17 GPa and 4.76 MPa $m^{1/2}$, which are 1.7 times and 1.5 times of those of the presintered ceramic, respectively, listed in Table II.

Of course, the disappearance of grain boundaries and voids is one of the main factors that increase the solidified eutectic ceramic mechanical property. Besides that, there are other key factors. The mechanical properties of two-phase Al_2O_3/ZrO_2 (Y_2O_3) eutectic are superior to that of either constituent alone due to strong constraining effects provided by the coherent interfaces and microstructure. The Al_2O_3/ZrO_2 (Y_2O_3) eutectic maintains a low energy interface resulting from directional solidification and can produce strong and stable reinforcing phase/matrix bonding.[30] The Al_2O_3 phase and the ZrO_2 phase present in the form of single crystal share an oxygen surface, and the two-phase interface is tightly bonded, and there is no amorphous phase which is easy to cause plastic deformation. The ZrO_2 phase is induced by stress to the phase transition. The bulk expansion and shear deformation due to phase transition absorb a large amount of energy, thus inhibiting the growth of microcracks, which makes the hardness and fracture toughness of the materials greatly improved.[31] The matrix and the ZrO_2 phase form an in situ composite pattern, where high elastic modulus ZrO_2 plays a reinforcing role, acting as crystal whiskers to reinforce the solidified ceramic.[32]

TABLE II. Mechanical properties of the eutectic ceramics.

	Hardness/GPa	Fracture toughness/MPa $m^{1/2}$
The presintered ceramic (1500 °C, 2 h)	9.51	3.17
The solidified ceramics (2200 °C, 3 mm/h)	16.17	4.76

IV. CONCLUSION

Directionally solidified eutectic ceramics are promising to be a new generation of ultra high temperature structural materials for aerospace engines. As the feed rod of the IHZM method, the presintered ceramic rod with as high density as possible was necessary to prepare high quality large solidified Al_2O_3/ZrO_2 eutectic ceramic. The preparation processing for the presintered ceramic rod was investigated via experiments at first. Then, some parameters of the IHZM process were optimized via numerical modeling. Next, an Al_2O_3/ZrO_2 eutectic ceramic rod with a diameter 10 mm was prepared with IHZM. And the mechanical properties of both the sintered and the solidified ceramics were tested, and the factors to improve the properties of the solidified ceramics were analyzed. The main conclusions are as follows:

(1) Increasing sintering temperature could increase the bulk density of presintered ceramics and decrease its porosity. Increasing sintering time had little effect on the

https://doi.org/10.1557/jmr.2018.113 Published online by Cambridge University Press

bulk density and the porosity. When the molding pressure increased, the bulk density increased first and then decreased, and the porosity increased first and then decreased.

(2) When the maximum temperature of the crucible wall was fixed, the saucer-shaped coil obtained a higher temperature gradient than the tubbiness coil; the increase in the number of turns of the saucer shaped coil could increase the melting zone height.

(3) In the directionally solidified Al_2O_3/ZrO_2 eutectic ceramics, the Al_2O_3 phase is the matrix phase, in which ZrO_2 phase embedded mostly with rod shape, and a little with lamellar. The hardness of directionally solidified eutectic ceramics reaches 16.17 GPa and the fracture toughness reaches 4.76 MPa $m^{1/2}$, which are 1.7 times and 1.5 times of the presintered eutectic ceramic, respectively.

(4) The disappearance of grain boundaries and voids, Al_2O_3 phase and ZrO_2 phase sharing an oxygen atom interface, and the uniform distribution of the ZrO_2 phase with higher elastic modulus in the matrix improve the solidified ceramic's mechanical properties.

ACKNOWLEDGMENTS

This work was financially supported by the National Natural Science Foundation of China (NSFC, Grant No. 51172161) and Natural Science Foundation of Shandong Province (Grant No. ZR2012EMM018).

REFERENCES

1. M. Attarian and A.K. Taheri: Microstructural evolution in creep aged of directionally solidified heat resistant HP-Nb steel alloyed with tungsten and nitrogen. *Mater. Sci. Eng., A* **659**, 104 (2016).
2. Y. Waku, N. Nakagawa, T. Wakamoto, H. Ohtsubo, K. Shimizu, and Y. Kohtoku: A ductile ceramic eutectic composite with high strength at 1873 K. *Nature* **389**, 49 (1997).
3. Y. Waku, N. Nakagawa, T. Wakamoto, H. Ohtsubo, K. Shimizu, and Y. Kohtoku: High temperature strength and thermal stability of a unidirectionally solidified eutectic composite. *J. Mater. Sci.* **33**, 1217 (1998).
4. Y. Waku, N. Nakagawa, T. Wakamoto, H. Ohtsubo, K. Shimizu, and Y. Kohtoku: The creep and thermal stability characteristics of a unidirectionally solidified eutectic composite. *J. Mater. Sci.* **33**, 4943 (1998).
5. Y. Waku, S. Sakata, A. Mitani, K. Shimizu, and M. Hasebe: Temperature dependence of flexural strength and microstructure of $Al_2O_3/Y_3Al_5O_{12}/ZrO_2$ ternary melt growth composites. *J. Mater. Sci.* **37**, 2975 (2002).
6. W. Ma, J. Zhang, H. Su, Q. Ren, B. Yao, and L. Liu: Microstructure transformation from irregular eutectic to complex regular eutectic in directionally solidified $Al_2O_3/GdAlO_3/ZrO_2$ ceramics by laser floating zone melting. *J. Eur. Ceram. Soc.* **36**, 1447 (2015).
7. O. Benamara, M. Cherif, T. Duffar, and K. Lebbou: Microstructure and crystallography of Al_2O_3–$Y_3Al_5O_{12}$–ZrO_2, ternary eutectic oxide grown by the micro pulling down technique. *J. Cryst. Growth* **429**, 27 (2015).
8. G. Liu, Q. Wang, J. Li, Y. Chen, and B. He: Preparation of Al_2O_3–ZrO_2–SiO_2, ceramic composites by high-gravity combustion synthesis. *Int. J. Refract. Met. Hard Mater.* **41**, 622 (2013).
9. L. Mei, P. Mai, J. Li, and K. Chen: Fabrication of nanostructure Al_2O_3/ZrO_2, (Y_2O_3) eutectic by combustion synthesis melt-casting under ultra-high gravity. *Mater. Lett.* **64**, 68 (2010).
10. H. Fu, J.L. Guo, and L. Liu: *Directional Solidification and Processing of Advanced Materials* (Science Press, Beijing, 2008).
11. B. Lu and Y. Zhang: Densification behavior and microstructure evolution of hot-pressed SiC–SiBCN ceramics. *Ceram. Int.* **41**, 8541 (2015).
12. F. Booth, L. Garrido, E. Aglietti, A. Silva, P. Pena, and C. Baudín: $CaZrO_3$–MgO structural ceramics obtained by reaction sintering of dolomite–zirconia mixtures. *J. Eur. Ceram. Soc.* **36**, 2611 (2016).
13. H. Yang, X. Zhou, J. Yu, H. Wang, and Z. Huang: Effect of microwave sintering time on the flexural properties of the SiC/SiC composites. *Ceram. Int.* **41**, 14692 (2015).
14. D.A. Jerebtsov, G.G. Mikhailov, and S.V. Sverdina: Phase diagram of the system: Al_2O_3–ZrO_2. *Ceram. Int.* **26**, 821 (2000).
15. P. Wang, H.B. Sun, J.H. Bai, and J.C. Liu: Investigation on solid-liquid interface morphology during the $A1_2O_3/MgA1_2O_4$ eutectic ceramics solidification. *J. Synth. Cryst.* **40**, 1252 (2011).
16. Y. Mizutani, H. Yasuda, I. Ohnaka, N. Maeda, and Y. Waku: Coupled growth of unidirectionally solidified Al_2O_3-YAG eutectic ceramics. *J. Cryst. Growth* **244**, 384 (2002).
17. C. Herring: Effect of change of scale on sintering phenomena. *J. Appl. Phys.* **21**, 301 (1950).
18. A.G. Balogh: Irradiation induced defect formation and phase transition in nanostructured ZrO_2. *Nucl. Instrum. Methods Phys. Res., Sect. B* **282**, 48 (2012).
19. M.H. Berger and A. Sayir: Directional solidification of Al_2O_3–Al_2TiO_5 system. *J. Eur. Ceram. Soc.* **28**, 2411 (2008).
20. M.C. Mesa, S. Serrano-Zabaleta, P.B. Oliete, and A. Larrea: Microstructural stability and orientation relationships of directionally solidified Al_2O_3–$Er_3Al_5O_{12}$–ZrO_2, eutectic ceramics up to 1600 °C. *J. Eur. Ceram. Soc.* **34**, 2071 (2014).
21. O. Khasanov, V. Osipov, E. Dvilis, A. Kachaev, A. Khasanov, and V. Shitov: Nanoscaled grain boundaries and pores, microstructure and mechanical properties of translucent Yb:[$Lu_xY_{(1-x)}O_3$] ceramics. *J. Alloys Compd.* **509**, S338–S342 (2011).
22. A. Ludwig and S. Leibbrandt: Generalized 'Jackson–Hunt' model for eutectic solidification at low and large Peclet numbers and any binary eutectic phase diagram. *Mater. Sci. Eng., A* **S375–377**, 540 (2004).
23. S. Akamatsu, S. Bottin-Rousseau, and G. Faivre: Determination of the Jackson–Hunt constants of the In–In_2Bi eutectic alloy based on in situ observation of its solidification dynamics. *Acta Mater.* **59**, 7586 (2011).
24. C. Stöcker and L. Ratke: A new 'Jackson–Hunt' model for monotectic composite growth. *J. Cryst. Growth* **203**, 582 (1999).
25. I. Barin and G. Platzki: *Thermochemical Data of Pure Substances* (VCH, Weinheim, 1989).
26. M. Gervais, S. Floch, J.C. Rifflet, J. Coutures, and J.P. Coutures: Effect of the melt temperature on the solidification process of liquid garnets $Ln_3Al_5O_{12}$ (Ln = Dy, Y, and Lu). *J. Am. Ceram. Soc.* **75**, 3166 (1992).
27. Y. Zheng, H. Li, T. Zhou, J. Zhao, and P. Yang: Microstructure and mechanical properties of Al_2O_3/ZrO_2 eutectic ceramic composites prepared by explosion synthesis. *J. Alloys Compd.* **551**, 475 (2013).
28. G.R. Anstis, P. Chantikul, B.R. Lawn, and D.B. Marshall: A critical evaluation of indentation techniques for measuring fracture toughness: I, direct crack measurements. *J. Am. Ceram. Soc.* **64**, 533 (1981).

https://doi.org/10.1557/jmr.2018.113 Published online by Cambridge University Press

29. Y.F. Deng, J. Zhang, H.J. Su, K. Song, L. Liu, and H.Z. Fu: Microstructure and fracture toughness of $A1_2O_3/Er_3A1_5O_{12}$ eutectic ceramic prepared by laser zone remelting. *J. Inorg. Mater.* **26**, 841 (2011).
30. A. Sayir and S.C. Farmer: The effect of the microstructure on mechanical properties of directionally solidified Al_2O_3/ZrO_2 (Y_2O_3) eutectic. *Acta Mater.* **48**, 4691 (2000).
31. W. Wang, Z. Liang, X. Han, J. Chen, C. Xue, and H. Zhao: Mechanical and thermodynamic properties of ZrO_2, under high-pressure phase transition: A first-principles study. *J. Alloys Compd.* **622**, 504 (2015).
32. S.Y. Zhai, J.C. Liu, and J. Wang: Microstructure of the directionally solidified ternary eutectic ceramic $Al_2O_3/MgAl_2O_4/ZrO_2$. *Ceram. Int.* **42**, 8079 (2016).

https://doi.org/10.1557/jmr.2018.113 Published online by Cambridge University Press